Available online on 15.11.2026 at http://jddtonline.info

Journal of Drug Delivery and Therapeutics

Open Access to Pharmaceutical and Medical Research

Copyright © 2026 The Author(s): This is an open-access article distributed under the terms of the CC BY-NC 4.0 which permits unrestricted use, distribution, and reproduction in any medium for non-commercial use provided the original author and source are credited

Open Access Full Text Article

Research Article

Short-Time Scale Molecular Dynamics and MM-GBSA Analysis of a Designed Acridone (ARB-373) in Complex with LSD1/KDM1A

Srimathi Dinakaran *[1], Tamilarasi G. [1], Gowtham K, [2]

[1] Department of Pharmaceutical Chemistry, College of Pharmacy, Madurai Medical College, Madurai, Tamil Nadu, India – 625020

[2] M. Pharm., Research Scholar, Department of Pharmacology, Mahatma Gandhi Medical College and Research Institute, Sri Balaji Vidyapeeth, Deemed to be University, Pondicherry

Article Info:

Article History:

Received 09 Aug 2026
Reviewed 24 Sep 2026
Accepted 15 Oct 2026
Published 15 Nov 2026

Cite this article as:

Srimathi D, Tamilarasi G, Gowtham K, Short-Time Scale Molecular Dynamics and MM-GBSA Analysis of a Designed Acridone (ARB-373) in Complex with LSD1/KDM1A, Journal of Drug Delivery and Therapeutics. 2026; 16(11):19-24 *DOI:* https://doi.org/10.22270/jddt.v16i11.8061

For Correspondence:

Srimathi Dinakaran, Department of Pharmaceutical Chemistry, College of Pharmacy, Madurai Medical College, Madurai, Tamil Nadu, India – 625020

Abstract

Objective: To examine, by all-atom molecular dynamics (MD) simulation, whether the docking-derived binding pose of ARB-373 a designed fluoro-cyano-benzyl acridone analogue of the natural product arborinine is retained over the accessible simulation window in the LSD1/KDM1A site and to obtain an exploratory implicit-solvent (MM-GBSA) estimate of the interaction energy of the complex. **Methods:** The top-ranked ARB-373 pose (AutoDock Vina 1.2.7; PDB 6TUY, FAD retained) was parameterised with AMBER99SB-ILDN (protein) and GAFF2/ACPYPE (ligand), solvated in TIP3P water and neutralised to 0.15 M NaCl. After energy minimisation and NVT/NPT equilibration, a 100 ps production simulation was run in GROMACS 2023 at 310 K and 1 bar (2 fs step, LINCS, PME, 1.0–1.2 nm cut-offs). Backbone and ligand RMSD, per-residue Cα RMSF, radius of gyration, SASA, intermolecular hydrogen bonds and minimum protein–ligand distance were analysed. The interaction energy was computed by single-trajectory MM-GBSA (Generalized Born, igb=5; 100 frames; no entropy term). **Results:** The simulated receptor was conformationally steady over the window (mean backbone RMSD 0.069 nm, plateau ≈0.09 nm; radius of gyration 1.667 ± 0.006 nm). Ligand RMSD tracked the backbone (≈0.07 nm) for the first ~48 ps, then rose to ≈0.22 nm and remained elevated, indicating that the ligand moved away from its docked pose; whether this reflects a genuine repositioning or a reorientation of the flexible N-benzyl group was not resolved. The minimum ligand–protein atom distance held at 0.206 ± 0.011 nm (≈2.1 Å), indicating continuous close contact but not, by itself, catalytic-pocket occupancy. Intermolecular hydrogen bonding was intermittent (0–1 bonds, mostly 0) and was not persistent even during the early pose-retained phase, so the docking-predicted Tyr761 hydrogen bond did not establish. Single-trajectory MM-GBSA gave ΔG(bind) ≈ −18.6 ± 2.3 kcal/mol, averaged across the pre- and post-transition geometries. **Conclusion:** Over 100 ps the simulated complex did not rapidly rearrange and the ligand did not exit, but the ligand did not remain in its docked pose and the averaged MM-GBSA value corresponds to no single state. The docked pose is therefore not supported as a structural hypothesis. These are preliminary, feasibility-level observations; extended, replicated simulation with positive and negative controls is required before any binding-mode, affinity or inhibition claim.

Keywords: LSD1; KDM1A; molecular dynamics; GROMACS; MM-GBSA; acridone; arborinine; binding-mode stability.

INTRODUCTION

Lysine-specific histone demethylase 1A (LSD1, also KDM1A) removes methyl groups from mono- and di-methylated lysine-4 of histone H3 and was the first enzyme shown to make histone methylation a reversible mark.[1] It is a flavin adenine dinucleotide (FAD) dependent amine oxidase whose substrate specificity is set by the complexes it resides in, principally the CoREST corepressor complex.[2] Aberrant LSD1 activity sustains the self-renewal programme of MLL-rearranged leukaemia stem cells[3] and the enzyme is over-expressed across several solid and haematological tumours, which has driven inhibitors into clinical evaluation.[4]

Many of the LSD1 inhibitors that have advanced to the clinic are irreversible, tranylcypromine-derived agents that form a covalent adduct with the flavin,[5] although reversible, non-covalent agents (for example seclidemstat) have also entered trials. Reversible chemotypes that occupy the substrate channel without modifying the cofactor remain of interest.[6] Arborinine, an acridone alkaloid from Glycosmis parva, is a candidate starting point: it is small and drug-like and has been reported to suppress clear-cell renal cell carcinoma through modulation of KDM1A/UBE2O signalling[7] (a cellular signalling study rather than a direct enzyme-inhibition assay). Its planar tricyclic core is geometrically compatible with the aromatic channel adjacent to the flavin.

ARB-373 is a designed arborinine analogue bearing fluorine at C-1, a cyano group at C-3 and a benzyl group at N-10. In the parent docking study it was the best-scoring member of a sixteen-compound series against the LSD1/CoREST structure PDB 6TUY, at −9.11 kcal/mol, versus −7.66 kcal/mol for arborinine. A gap of this size (≈1.5 kcal/mol) is within the typical uncertainty of empirical docking scores and is not, by itself, strong evidence of improved affinity.

A docking score is a single-point estimate for a single rigid-receptor pose and carries no information about whether that pose is retained at physiological temperature; empirical scoring functions frequently rank non-native poses above native ones. Molecular dynamics provides a partial test a solvated, thermostatted trajectory can reveal whether a predicted geometry is immediately unstable and supplies the configurational ensemble that end-point methods such as MM-GBSA require,[9] although reliable binding-mode and affinity assessment requires far longer sampling than is reported here.

OBJECTIVES

The study had two limited objectives: (i) to observe, over the accessible 100 ps window, whether the docking-derived pose of ARB-373 is retained in the simulated LSD1/KDM1A system and to document any change in the ligand's position; and (ii) to obtain an exploratory single-trajectory MM-GBSA interaction energy for the complex. Establishing the equilibrium binding mode or a converged binding free energy is beyond a single short trajectory and is not claimed.

MATERIALS AND METHODS

Origin of the simulated pose

Starting coordinates were obtained from rigid-receptor docking performed in a companion study and are summarised here only as provenance. The receptor was the human LSD1/CoREST crystal structure PDB 6TUY (2.6 Å)[17], with the FAD cofactor retained because the isoalloxazine ring forms the floor of the catalytic pocket. Docking used AutoDock Vina 1.2.7.[10,11] In protocol validation, redocking of the co-crystallised ligand NY8 reproduced the crystallographic geometry to a heavy-atom RMSD of 0.15 Å; this near-native pose was not the single top-scoring pose (−10.09 kcal/mol) but a lower-ranked pose (−9.17 kcal/mol) lying within the energy window. For ARB-373, the top-scoring pose (−9.11 kcal/mol) was used as the MD input.

System preparation

The simulated system comprised the LSD1 catalytic domain with FAD retained and ARB-373 in the docked pose. ARB-373 was treated as a neutral acridone, consistent with the amide-like character of its N-10 nitrogen at physiological pH. Protein atoms were assigned AMBER99SB-ILDN parameters[12]; ligand parameters were generated with GAFF2 through ACPYPE.[13,14] The complex was solvated with TIP3P water[15] in a dodecahedral box (1.0 nm minimum solute–wall distance), neutralised and brought to 0.15 M NaCl.

Minimisation, equilibration and production

Simulations were run in GROMACS 2023.[8] After energy minimisation, the system was equilibrated under NVT then NPT before production. Production used the leap-frog integrator at a 2 fs timestep with LINCS constraints on bonds to hydrogen, a Verlet scheme, particle-mesh Ewald electrostatics (1.2 nm real-space cut-off) and a van der Waals force-switch between 1.0 and 1.2 nm, with velocity-rescaling (310 K) and Parrinello–Rahman (1 bar) coupling. The production trajectory ran for 100 ps.

Trajectory analysis

Periodic-boundary artefacts were removed before analysis. Backbone and ligand RMSD, per-residue Cα RMSF, radius of gyration, total SASA, intermolecular hydrogen-bond count and minimum protein–ligand distance were computed with the GROMACS tools. Because the production window is 100 ps, no portion was discarded as equilibration and all means are computed over the full window; given the early radius-of-gyration drift, these means should be read as provisional.

Interaction-energy estimate (MM-GBSA)

The interaction energy was estimated by the single-trajectory MM-GBSA approach over 100 frames, using the Generalized Born implicit-solvent model igb=5 at 0.15 M salt, with no entropy term.[9,16] The reported quantity is therefore an effective enthalpy computed with a GB model, suitable at best for relative ranking within a congeneric series under an identical protocol, not an absolute binding free energy.

RESULTS

The simulated receptor is conformationally steady over the window

Protein backbone RMSD rose over the first few picoseconds and reached a plateau near 0.09 nm (peaking at ≈0.092 nm), with a mean of ≈0.069 nm (Figure 1A, red trace). The radius of gyration stayed at 1.667 ± 0.006 nm after an initial rise over the first ~15–30 ps (Figure 1C). Total SASA fluctuated between ≈89 and 94 nm^2 with a modest upward drift over the second half of the run (Figure 1D). Per-residue Cα RMSF stayed between 0.035 and 0.125 nm, largest at the chain termini and in loop regions (Figure 1B). These metrics indicate that the simulated system did not undergo large, rapid rearrangement over the window. They do not establish thermodynamic stability or correct maintenance of the fold over biologically relevant times, both of which are beyond a 100 ps trajectory.

The ligand moves away from its docked pose at approximately 48 ps

Ligand RMSD did not track the backbone (Figure 1A orange trace). For the first ~48 ps it fluctuated around 0.07 nm; at ~48 ps it rose to ≈0.20 nm and then held near 0.22 nm (0.19–0.26 nm) for the remaining ~50 ps without returning to its initial value. An increase of this magnitude (~1.5 Å) is modest and is consistent with either a genuine repositioning of the ligand within the

site or a reorientation of the flexible N-benzyl substituent while the acridone core remains in place. Distinguishing these requires core-only versus substituent RMSD, torsion analysis, pose clustering, contact maps and representative structures before and after the transition, none of which were performed here. The data therefore show that the ligand departed its initial pose, but do not establish a specific, distinct second binding mode. The ligand did not dissociate: the minimum distance between any ligand atom and any protein atom held at 0.206 ± 0.011 nm throughout (Figure 1F).

The minimum-distance metric

The reported 0.206 ± 0.011 nm is a minimum atom–atom distance (≈2.1 Å). At this value it is shorter than a heavy-atom van der Waals contact (~3.4–4.0 Å) and is consistent with a hydrogen-involving or close polar contact rather than with heavy-atom packing. A minimum distance to any protein atom does not by itself establish that the ligand remained in the catalytic pocket a surface-bound ligand could give a similar value. Centre-of-mass distance to the pocket and specific residue-contact analysis would be needed to establish site occupancy and were not performed.

Hydrogen bonding is intermittent

The intermolecular hydrogen-bond count alternated between zero and one and was zero for most frames, including almost all of the final 10 ps (Figure 1E). It was not persistent even during the early (0–~45 ps) pose-retained phase, so the Tyr761 hydrogen bond (2.7 Å) assigned in the docked pose was never a persistent feature of the simulated complex. As simulated, any association is dominated by shape and dispersion contacts rather than by directional hydrogen bonding.

Interaction-energy estimate

Single-trajectory MM-GBSA over 100 frames returned a favourable interaction energy (Table 1).

Table 1. Single-trajectory MM-GBSA interaction-energy summary for the simulated LSD1 (KDM1A)–ARB-373 complex. Values are effective enthalpies (no entropy term); the ± values are standard deviations across frames, not standard errors.

Term	Value (kcal/mol)
ΔE_MM (gas-phase molecular mechanics)	−28.5 ± 1.9
ΔG_solv (GB + non-polar)	+9.9 ± 0.9
ΔG_bind (effective, MM-GBSA)	−18.6 ± 2.3

Because the 100 frames were drawn across the whole trajectory, this value averages the pre- and post-transition geometries and corresponds to neither state individually. The ± is a standard deviation over strongly autocorrelated frames (1 ps spacing), not a standard error. Separate MM-GBSA estimates for the 0–48 ps and ~52–100 ps windows, with per-residue decomposition, would be the appropriate exploratory analysis and were not performed here.

Table 2. Summary of trajectory metrics over the 100 ps production window.

Metric	Value	Reading
Production length	100 ps	Preliminary; see Limitations
Mean backbone RMSD	0.069 nm (plateau ≈0.09 nm)	No large rapid rearrangement
Ligand RMSD, 0–48 ps	≈0.07 nm	Docked pose initially retained
Ligand RMSD, 48–100 ps	≈0.22 nm	Moved from docked pose
Radius of gyration	1.667 ± 0.006 nm	Stable over window
SASA	≈89–94 nm^2, slight upward drift	No large exposure change
Cα RMSF range	0.035–0.125 nm	Termini/loops most mobile
Intermolecular H-bonds	0–1, mostly 0	No persistent H-bond
Min. ligand–protein atom distance	0.206 ± 0.011 nm (≈2.1 Å)	Close contact; not proof of pocket occupancy
MM-GBSA ΔG_bind (effective)	−18.6 ± 2.3 kcal/mol	Ensemble-averaged; relative use only

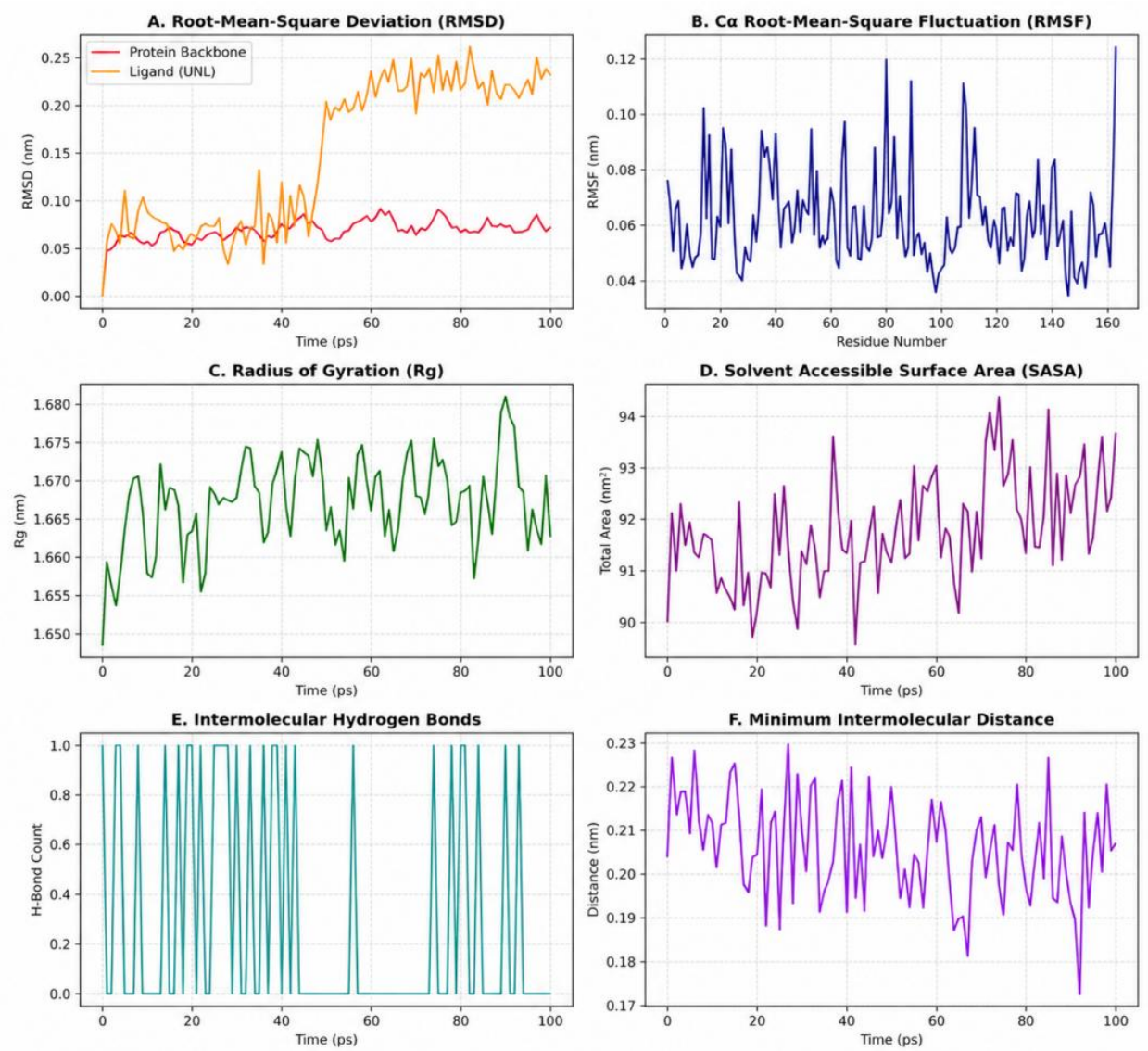


Figure 1. Trajectory analysis of the simulated LSD1 (KDM1A)–ARB-373 complex over the 100 ps window. (A) Protein backbone RMSD (red) and ligand RMSD (orange); the ligand tracks the backbone until ~48 ps, then rises to a higher plateau near 0.22 nm. (B) Per-residue Cα RMSF (x-axis spans ~163 residues; see Limitations). (C) Radius of gyration, 1.667 ± 0.006 nm after an initial rise. (D) Total SASA, with a slight upward drift. (E) Intermolecular hydrogen-bond count, 0–1 and mostly 0 throughout. (F) Minimum ligand–protein atom distance, 0.206 ± 0.011 nm.

DISCUSSION

What a 100 ps window can and cannot establish

A 100 ps trajectory samples a narrow slice of configurational space. It can reveal fast events immediate pose instability, a ligand that exits at once or gross early rearrangement but it cannot characterise an equilibrium binding mode, sample pocket side-chain rearrangement or converge an end-point energy. Binding-mode and affinity assessment conventionally requires at least 100 ns and commonly hundreds of nanoseconds in independent replicates, which is two to three orders of magnitude more sampling than reported here. The low backbone-RMSD plateau indicates only that the starting structure did not rearrange rapidly on this timescale; it is not evidence of thermodynamic stability and much of the plateau value reflects initial relaxation rather than equilibrium behaviour.

Interpreting the ligand movement

The rise in ligand RMSD at ~48 ps, with an unbroken minimum-distance trace, shows the ligand moving from its docked geometry while remaining in contact. At least three readings are consistent with the data and cannot be separated at 100 ps with a single replica: a scoring-function artefact in the initial docked pose (the companion study's own validation showed the top-scoring NY8 pose, −10.09 kcal/mol, was not the geometry-reproducing pose, −9.17 kcal/mol); a genuine early relaxation into a nearby minimum; or a reorientation of the flexible N-benzyl substituent with the core essentially fixed. Deciding among these requires the decomposed-RMSD, clustering and torsion analyses noted above. What can be said is that the docked pose is not retained for most of the window and should not be advanced as a structural hypothesis.

The hydrogen-bonding and interaction-energy results

Docking assigned ARB-373 a 2.7 Å hydrogen bond to Tyr761, but the trajectory shows at most one intermolecular hydrogen bond and none across most frames including the early pose-retained phase so this contact was never persistent as simulated. The MM-GBSA value (ΔG_bind ≈ −18.6 ± 2.3 kcal/mol) is favourable in sign and unremarkable in shape, but carries three qualifications: it omits configurational entropy and is therefore an effective enthalpy that overestimates absolute affinity; the single-trajectory approximation assumes bound and free states sample the same conformations;[9] and the frames span two structurally distinct geometries, so the number corresponds to neither alone. It is usable only for relative ranking within a congeneric series under an identical protocol.

LIMITATIONS

This work is a preliminary computational study and its claims are bounded by the following limitations, several of which also indicate the reporting and analysis that a full study should add.

1. Simulated construct. The global metrics (radius of gyration 1.667 nm; total SASA ≈90 nm^2) are consistent with a system of ~160–200 residues, matching the ~163-residue span of the Cα RMSF axis. The exact simulated construct chain(s), residue range, any missing residues, whether the CoREST chain of 6TUY was included and whether the complete catalytic pocket, FAD environment and Tyr761 are present should be stated explicitly and Figure 1B regenerated with absolute residue numbering. The receptor-steadiness result applies to the system as simulated.

2. Force-field and preparation reporting. Full parameterisation details should accompany the work: the FAD charges, atom types, topology and protonation state (AMBER99SB-ILDN contains no FAD parameters); the ARB-373 SMILES, tautomer, net charge and charge-derivation method; and the water and ion counts and total atom count.

3. Free-energy method. igb=5 selects a Generalized Born model, so the calculation is MM-GBSA. No Poisson–Boltzmann calculation is reported; no entropy term was included (the value is an effective enthalpy); frames at 1 ps spacing are strongly autocorrelated, so the quoted ± is a standard deviation and not a standard error and block averaging was not applied; and the estimate averages two structurally distinct geometries. The value is suitable only for relative ranking under an identical protocol.

4. Timescale, replicates and controls. The 100 ps window is two to three orders of magnitude short of conventional binding-mode validation. A single trajectory from one set of initial velocities was run, so the ~48 ps event cannot be shown reproducible and neither arborinine nor the native ligand NY8 was simulated under the same protocol as a control.

5. Equilibration and analysis specification. NVT/NPT durations and restraint schedules are not reported; the early radius-of-gyration drift suggests ongoing relaxation and no equilibration window was discarded. The RMSD fitting groups, the atom selections for ligand RMSD and for the minimum-distance calculation (in particular whether hydrogens were included), the hydrogen-bond distance/angle criteria and the SASA probe radius should also be stated.

6. Docking provenance. The redock RMSD of the native ligand (reported as 0.15 Å) should be read with caution and confirmed and the ARB-373 starting pose was the top-scoring pose rather than a geometry-validated one.

7. Structural evidence and experimental validation. A distinct second bound orientation is not claimed, as decomposed-RMSD, clustering and torsion analyses were not performed. A metric reported in the source as a secondary-structure residue count could not be interpreted unambiguously and was omitted. The computational data do not establish inhibition of LSD1 by ARB-373; all claims are restricted to computational observations.

CONCLUSION

Within a 100 ps simulation, the modelled LSD1–ARB-373 system did not undergo large rapid rearrangement and the ligand did not dissociate, but the ligand moved away from its docking-derived pose at ~48 ps, the predicted Tyr761 hydrogen bond was never persistent and the single-trajectory MM-GBSA value (≈−18.6 kcal/mol, effective enthalpy) averages two distinct geometries and corresponds to none. The supportable result is therefore minimal and preliminary: the docked pose is not retained and should not be advanced as a structural hypothesis. Extending the work to at least 100 ns in independent replicates, with arborinine and NY8 as controls and entropy-corrected, block-averaged energetics, is required before any binding-mode, affinity or inhibition claim. As it stands, the study is best regarded as a preliminary computational feasibility note.

Data and Code Availability: The production parameter files, topologies, trajectory and analysis outputs are available from the corresponding author on reasonable request.

Acknowledgements: The authors thank the College of Pharmacy, Madurai Medical College, Madurai, for the infrastructural facilities provided for this work.

Conflict Of Interest: The authors declare no conflict of interest.

REFERENCES

1. Shi Y, Lan F, Matson C, Mulligan P, Whetstine JR, Cole PA, Casero RA, Shi Y. Histone demethylation mediated by the nuclear amine oxidase homolog LSD1. Cell. 2004;119(7):941-953. https://doi.org/10.1016/j.cell.2004.12.012 PMid:15620353
2. Forneris F, Binda C, Battaglioli E, Mattevi A. LSD1: oxidative chemistry for multifaceted functions in chromatin regulation. Trends Biochem Sci. 2008;33(4):181-189. https://doi.org/10.1016/j.tibs.2008.01.003 PMid:18343668

3. Harris WJ, Huang X, Lynch JT, Spencer GJ, Hitchin JR, Li Y, et al. The histone demethylase KDM1A sustains the oncogenic potential of MLL-AF9 leukemia stem cells. Cancer Cell. 2012;21(4):473-487. https://doi.org/10.1016/j.ccr.2012.03.014 PMid:22464800

4. Fang Y, Liao G, Yu B. LSD1/KDM1A inhibitors in clinical trials: advances and prospects. J Hematol Oncol. 2019;12(1):129. https://doi.org/10.1186/s13045-019-0811-9 PMid:31801559 PMCid:PMC6894138

5. Schmidt DMZ, McCafferty DG. trans-2-Phenylcyclopropylamine is a mechanism-based inactivator of the histone demethylase LSD1. Biochemistry. 2007;46(14):4408-4416. https://doi.org/10.1021/bi0618621 PMid:17367163

6. Vianello P, Sartori L, Amigoni F, Cappa A, Faga G, Fattori R, et al. Thieno[3,2-b]pyrrole-5-carboxamides as new reversible inhibitors of histone lysine demethylase KDM1A/LSD1. Part 2. J Med Chem. 2017;60(5):1693-1715. https://doi.org/10.1021/acs.jmedchem.6b01019 PMid:28186757

7. Feng C, Gong L, Wang J. Arborinine from Glycosmis parva leaf extract inhibits clear-cell renal cell carcinoma by inhibiting KDM1A/UBE2O signaling. Food Nutr Res. 2022;66:8714. https://doi.org/10.29219/fnr.v66.8714 PMid:36185617 PMCid:PMC9487452

8. Abraham MJ, Murtola T, Schulz R, Páll S, Smith JC, Hess B, Lindahl E. GROMACS: high performance molecular simulations through multi-level parallelism from laptops to supercomputers. SoftwareX. 2015;1-2:19-25. https://doi.org/10.1016/j.softx.2015.06.001

9. Genheden S, Ryde U. The MM/PBSA and MM/GBSA methods to estimate ligand-binding affinities. Expert Opin Drug Discov. 2015;10(5):449-461. https://doi.org/10.1517/17460441.2015.1032936 PMid:25835573

10. Trott O, Olson AJ. AutoDock Vina: improving the speed and accuracy of docking with a new scoring function, efficient optimization and multithreading. J Comput Chem. 2010;31(2):455-461. https://doi.org/10.1002/jcc.21334 PMid:19499576

11. Eberhardt J, Santos-Martins D, Tillack AF, Forli S. AutoDock Vina 1.2.0: new docking methods, expanded force field and Python bindings. J Chem Inf Model. 2021;61(8):3891-3898. https://doi.org/10.1021/acs.jcim.1c00203 PMid:34278794

12. Lindorff-Larsen K, Piana S, Palmo K, Maragakis P, Klepeis JL, Dror RO, Shaw DE. Improved side-chain torsion potentials for the Amber ff99SB protein force field. Proteins. 2010;78(8):1950-1958. https://doi.org/10.1002/prot.22711 PMid:20408171

13. Wang J, Wolf RM, Caldwell JW, Kollman PA, Case DA. Development and testing of a general amber force field. J Comput Chem. 2004;25(9):1157-1174. https://doi.org/10.1002/jcc.20035 PMid:15116359 PMCid:PMC12795828

14. Sousa da Silva AW, Vranken WF. ACPYPE - AnteChamber PYthon Parser interfacE. BMC Res Notes. 2012;5:367. https://doi.org/10.1186/1756-0500-5-367 PMid:22824207

15. Jorgensen WL, Chandrasekhar J, Madura JD, Impey RW, Klein ML. Comparison of simple potential functions for simulating liquid water. J Chem Phys. 1983;79(2):926-935. https://doi.org/10.1063/1.445869

16. Miller BR 3rd, McGee TD Jr, Swails JM, Homeyer N, Gohlke H, Roitberg AE. MMPBSA.py: an efficient program for end-state free energy calculations. J Chem Theory Comput. 2012;8(9):3314-3321. https://doi.org/10.1021/ct300418h PMid:26605738 PMCid:PMC11413209

17. Berman HM, Westbrook J, Feng Z, Gilliland G, Bhat TN, Weissig H, Shindyalov IN, Bourne PE. The Protein Data Bank. Nucleic Acids Res. 2000;28(1):235-242. https://doi.org/10.1093/nar/28.1.235 PMid:10592235

18. Valdés-Tresanco MS, Valdés-Tresanco ME, Valiente PA, Moreno E. gmx_MMPBSA: a new tool to perform end-state free energy calculations with GROMACS. J Chem Theory Comput. 2021;17(10):6281-6291. https://doi.org/10.1021/acs.jctc.1c00645 PMid:34586825